The EMBO Journal Vol.19 No.7 pp.1691–1702, 2000

A novel SMC protein complex in *Schizosaccharomyces pombe* contains the Rad18 DNA repair protein

Maria I.Fousteri and Alan R.Lehmann[1]

MRC Cell Mutation Unit, University of Sussex, Falmer, Brighton BN1 9RR, UK

[1]Corresponding author
e-mail: a.r.lehmann@sussex.ac.uk

In *Schizosaccharomyces pombe*, *rad18* is an essential gene involved in the repair of DNA damage produced by ionizing radiation and in tolerance of UV-induced DNA damage. The Rad18 protein is a member of the SMC (structural maintenance of chromosomes) superfamily, and we show that, like the other SMC proteins in condensin and cohesin, Rad18 is a component of a high-molecular-weight complex. This complex contains at least six other proteins, the largest of which is Spr18, a novel SMC family member closely related to Rad18, and likely to be its heterodimeric partner. SMC proteins have ATP-binding domains at the N- and C-termini, and two extended coiled-coil domains separated by a hinge in the middle. We show that the N-terminal ATP-binding domain of Rad18 is essential for all functions, and overexpression of an N-terminal mutant has a dominant-negative effect. We have identified an important mutation (S1045A) near the C-terminus of Rad18 that separates its repair and essential roles. Potential models for the role of the Rad18–Spr18 complex during DNA repair are discussed.

Keywords: ATPase/coiled coils/DNA repair/fission yeast/SMC proteins

Introduction

Many genes involved in the response to DNA damage have been identified in the fission yeast *Schizosaccharomyces pombe* (see Lehmann, 1996). Epistasis analysis has enabled these genes to be assigned to different DNA repair pathways. Following treatment with ionizing radiation, repair of DNA double-strand breaks requires genes known to be involved in homologous recombination, suggesting that this mechanism is likely to be the major means of repairing such DNA damage in fission yeast. Photoproducts induced in DNA by UV-irradiation can be repaired both by the classical nucleotide excision repair (NER) system, which is conserved in all eukaryotes, and by a second excision repair process, which is specific to *S.pombe* and a few other organisms (Yonemasu *et al*., 1997; Yasui and McCready, 1998). In addition to these pathways that repair DNA damage directly, cells are able to tolerate UV damage during DNA replication (Murray *et al*., 1997) and to utilize cell cycle checkpoint mechanisms to ameliorate the deleterious effects of DNA damage by arresting the cell cycle following damaging treatments (for review, see Caspari and Carr, 1999).

In previous work we used the *rad18-X* mutant to show that the Rad18 protein was involved in repair of ionizing radiation damage (Lehmann *et al*., 1995). Double-strand breaks are the principal lesions responsible for killing cells by ionizing radiation. Both Verkade *et al*. (1999) and we (unpublished observations) have shown that *rad18-X* cells are deficient in repair of radiation-induced double-strand breaks.

Epistasis analysis in response to UV-irradiation suggests that Rad18 is not involved in NER, but that it does play a role in the second excision repair pathway for UV damage. The first step in this pathway is mediated by UV damage-endonuclease (UVDE) (Yonemasu *et al*., 1997), which nicks UV-irradiated DNA on the 5′ side of UV photoproducts (Avery *et al*., 1999; Yoon *et al*., 1999). In a *uvde* background, the *rad18-X* mutation still sensitized the cells to UV-irradiation (Yonemasu *et al*., 1997), and further epistasis analysis suggested that this was due to a role for Rad18 in a DNA damage tolerance pathway (Murray *et al*., 1997). Furthermore, deletion of the *rad18* gene demonstrated that it was essential for cell proliferation, and our data led us to propose tentatively that this essential role was an involvement in DNA replication (Lehmann *et al*., 1995). Figure 1 summarizes the pathways in which Rad18 is involved, based on this genetic analysis.

Sequence analysis of Rad18 (Lehmann *et al*., 1995) showed that the 131 kDa Rad18 protein was a member of the SMC (structural maintenance of chromosomes) superfamily. SMC proteins have globular N- and C-terminal domains, which are involved in ATP and Mg^{2+} binding, and two extended α-helical coiled-coil domains involved in protein–protein interactions, separated by a hinge region (for reviews, see Hirano, 1998, 1999; Jessberger *et al*., 1998). Recent work using *Saccharomyces cerevisiae*, *S.pombe* and *Xenopus laevis* has identified two protein complexes containing heterodimeric pairs of SMC proteins. Smc2 and Smc4 (and their orthologues) form the core of condensin, a five-subunit complex involved in chromosome condensation (Hirano *et al*., 1997; Sutani *et al*., 1999). Smc1 and Smc3 (and their orthologues) are the core of a five-subunit cohesin complex, which is required for sister chromatid cohesion (Michaelis *et al*., 1997; Losada *et al*., 1998). There is also evidence from bovine cells to suggest that SMC1 and SMC3 proteins form part of a complex with DNA ligase III and DNA polymerase ε, which has DNA strand exchange activity (Jessberger *et al*., 1996).

We describe in this paper the purification of a high-molecular-weight complex with DNA-dependent ATPase activity, which contains Rad18 and at least six other polypeptides. The largest of these is a novel SMC protein (Spr18), which is likely to be the heterodimeric partner

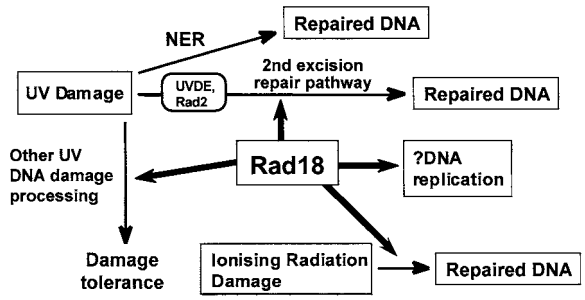

Fig. 1. Involvement of Rad18 in different cellular responses to DNA damage.

of Rad18. We show by site-directed mutagenesis that the N-terminal ATP-binding domain of Rad18 is required for all its functions, and that a C-terminal mutation can separate repair from essential functions.

Results

Rad18 is part of a high-molecular-weight complex

To determine whether Rad18, like other SMC proteins, is a member of a protein complex, we fractionated extracts of *S.pombe* in gel filtration columns. For these experiments we constructed cell strain myc-Rad18, in which the *rad18* gene was *myc*-tagged in the genome at the 5′ end, remaining under the control of its own promoter. When extracts of myc-Rad18 cells were passed down a Superdex 200 column, all the Rad18 protein was found in a high-molecular-weight peak (M_r >700 kDa). To obtain a more accurate estimate of the size of this complex, the peak fractions from the column were pooled and analysed on a Superose 6 column (Figure 2A). The results show that Rad18 is part of a complex whose apparent M_r is ~1.6 MDa. This complex was stable in the presence of up to 0.7 M NaCl (not shown). Using a polyclonal antibody raised against a Rad18 peptide, we also showed that the gel filtration profile was identical whether or not the Rad18 protein was N-terminally myc-tagged (Figure 2A and B). No change in the gel filtration profile was detected when extracts of γ-irradiated cells were used (data not shown).

As discussed below, the mutation in *rad18-X* is located in the hinge region, immediately adjacent to the second coiled-coil region (see Figure 5A). This raised the possibility that the mutation might disrupt the coiled-coil structure of the protein and interfere with complex formation. The Rad18 profiles on gel filtration columns using normal and *rad18-X* extracts were, however, indistinguishable (compare Figure 2C and A), even at salt concentrations up to 0.7 M NaCl. The *rad18-X* mutation does not, therefore, interfere with complex formation.

Purification of Rad18

We have developed a purification procedure for the Rad18-containing complex, using extracts from myc-Rad18 cells (Figure 3A). After ammonium sulfate precipitation, the extracts were subjected to gel filtration on Superdex 200. The high-molecular-weight fractions containing Rad18 were pooled and fractionated on a heparin–Sepharose column. The 0.6 M KCl fractions, which contained the Rad18 protein, were incubated with protein G beads covalently cross-linked to anti-myc antibody. After extensive washing, bound proteins were eluted with a peptide corresponding to the c-*myc* epitope, and analysed both by immunoblotting and colloidal Coomassie staining. Immunoblotting showed that the bound and eluted proteins contained myc-tagged Rad18 (Figure 3B, lane 2). When extracts from untagged control cells (strain 501) were subjected to identical purification procedures, no corresponding protein was bound to the beads (Figure 3B, lane 4). Coomassie staining revealed that, apart from Rad18, there were six specific bands in the eluate from the tagged cells (Figure 3C, lane 3) that were not found in similar experiments using untagged control cells (Figure 3C, lanes 1 and 2). One of these specific bands, p124, had a molecular weight close to that of Rad18 and was of similar intensity.

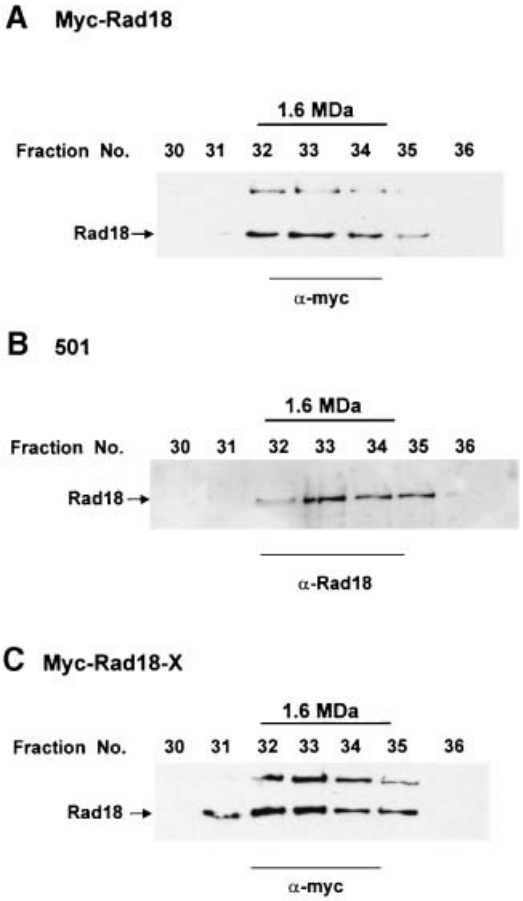

Fig. 2. Rad18 is part of a high-molecular-weight complex. Extracts of myc-Rad18 (**A**) or myc-Rad18-X cells (**C**) were precipitated with ammonium sulfate, fractionated on Superdex 200 and the high-molecular-weight peak analysed by gel filtration on a Superose 6 column. Fractions were subjected to immunoblotting with anti-myc antibody. The high-molecular-weight band on the gel is non-specific cross-reacting material. (**B**) Wild-type strain 501 was subjected to the same treatment as above, but analysed with anti-Rad18 antibody.

ATPase activity

Mutagenesis studies described in detail below implicate ATP-binding activity of Rad18 in all its functions, suggesting that the protein might have ATPase activity. We have therefore measured ATPase activity of the Rad18 complex. We assayed the peptide eluate from the immunoaffinity beads for ATPase activities in the presence and

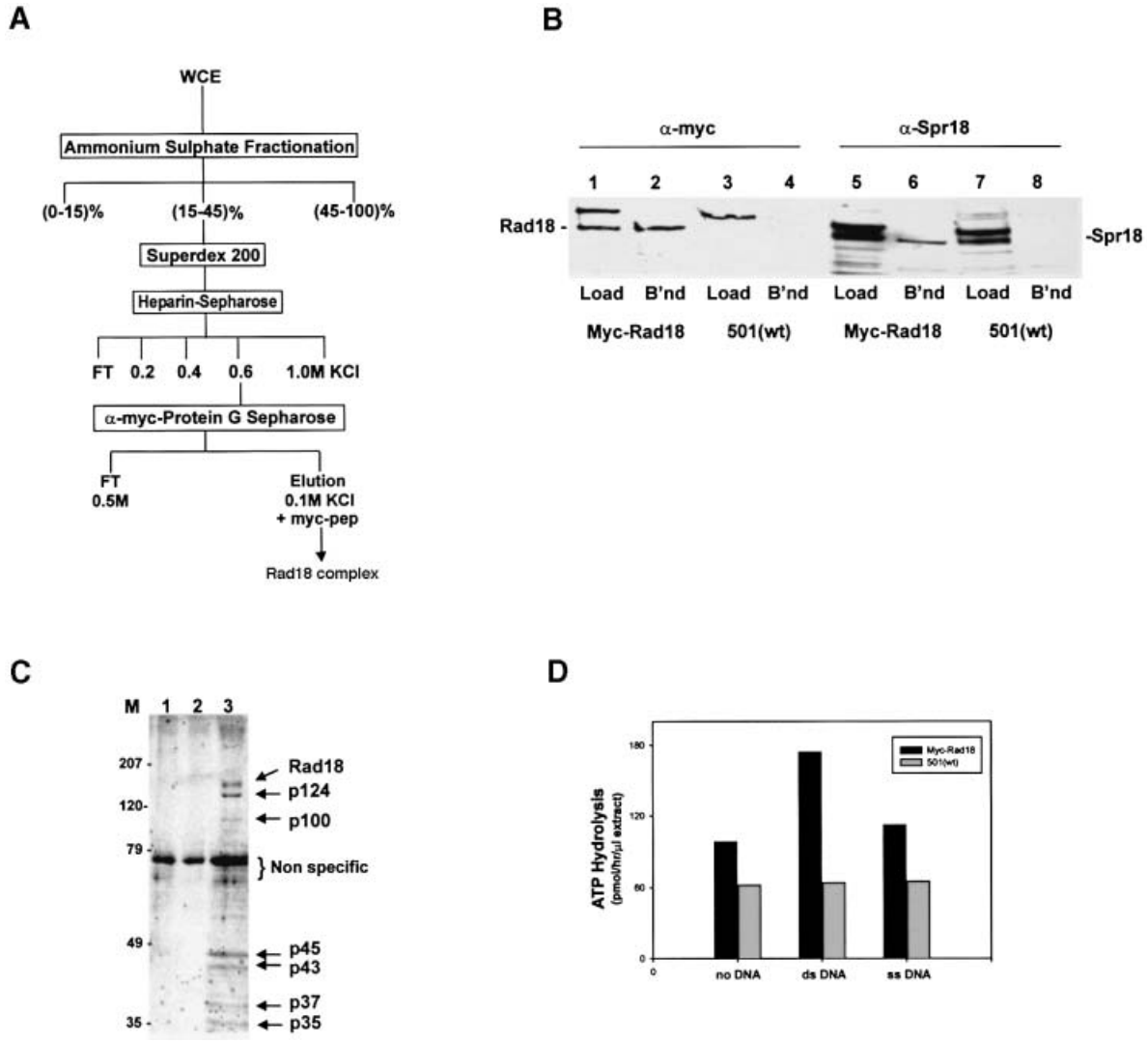

Fig. 3. The Rad18 complex. (**A**) Scheme for purification of the Rad18 complex from myc-Rad18 cell extracts (WCE, whole cell extracts; FT, flow-through). (**B**) Samples of the proteins loaded onto (Load) and eluted from (B'nd) the anti-myc immuno-affinity beads were immunoblotted with anti-myc or anti-Spr18 antibodies. (**C**) Proteins bound to the beads were eluted with the myc peptide and analysed by SDS–PAGE. The gel was fixed and stained with colloidal Coomassie Blue. Lanes 1 and 2, two extracts of strain 501; lane 3, myc-Rad18. (**D**) ATPase activity of the Rad18 complex. Experiments were carried out three times, typical results are shown.

absence of DNA. Eluate from the myc-Rad18 cell extracts had significant ATPase activity, which was stimulated by single-stranded, and to a greater extent by double-stranded DNA (Figure 3D). In contrast, eluate from untagged control strain 501 containing an equal amount of the non-specific 73 kDa protein (see Figure 3C) had minimal activity, which was unchanged by the addition of DNA. The complex is therefore associated with specific DNA-stimulated ATPase activity.

Spr18, a heterodimeric partner of Rad18

In the SMC family, Smc2 and Smc4 form a heterodimeric component of the condensin complex (Hirano *et al*., 1997), which is involved in chromosome condensation. Smc1 and Smc3 are similarly part of cohesin, involved in sister chromatid cohesion (Michaelis *et al*., 1997). We therefore anticipated that Rad18 might have a heterodimeric partner, and we considered the possibility that the p124 polypeptide in the complex might be a novel SMC protein partner of Rad18. We searched the *S.pombe* sequence database and found a candidate open reading frame (ORF) in cosmid C14C4 from chromosome 1 (DDBJ/EMBL/GenBank accession No. Z98596) with an orthologue in the *S.cerevisiae* database (ORF SCYOL034W; DDBJ/EMBL/GenBank accession No. Z74776). The predicted 123 kDa protein was related to the SMC family, but was most closely related to Rad18 (see Figure 4A). We designated it Spr18 (SMC partner of rad18). Alignments of Rad18 with Spr18 and its *S.cerevisiae* orthologue are shown in Figure 4B. There is 28% identity between the *S.pombe* and *S.cerevisiae* orthologues, and 20% identity between Rad18 and Spr18. Like *rad18*, *spr18* has a small intron (49 bases) close to the 5′ end of the gene (between nt 187 and 188).

In order to determine whether Spr18 interacts with Rad18 *in vivo*, we carried out immunoprecipitations using the myc-Rad18 strain (Figure 4C). Extracts were immunoprecipitated with antibody directed against a peptide from Spr18 (Figure 4C, lanes 2, 4, 6 and 8) or, as control, with anti-myc antibody (lanes 1, 3, 5 and 7). The immuno-

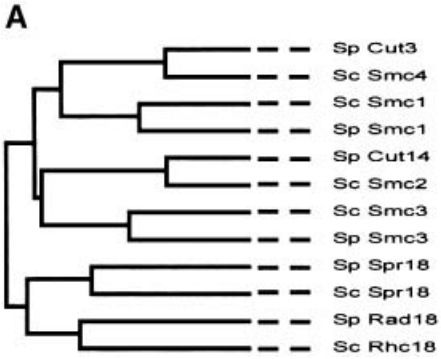
A
Sp Cut3
Sc Smc4
Sc Smc1
Sp Smc1
Sp Cut14
Sc Smc2
Sc Smc3
Sp Smc3
Sp Spr18
Sc Spr18
Sp Rad18
Sc Rhc18

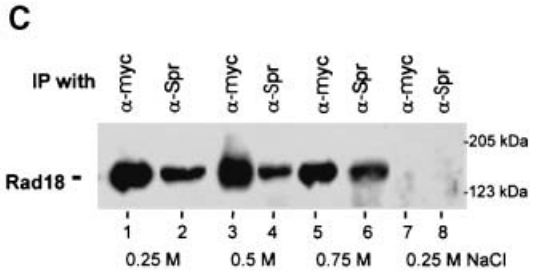
C
IP with
α-myc
α-Spr
α-myc
α-Spr
α-myc
α-Spr
α-myc
α-Spr
Rad18
205 kDa
123 kDa
1 2 3 4 5 6 7 8
0.25 M
0.5 M
0.75 M
0.25 M NaCl

B

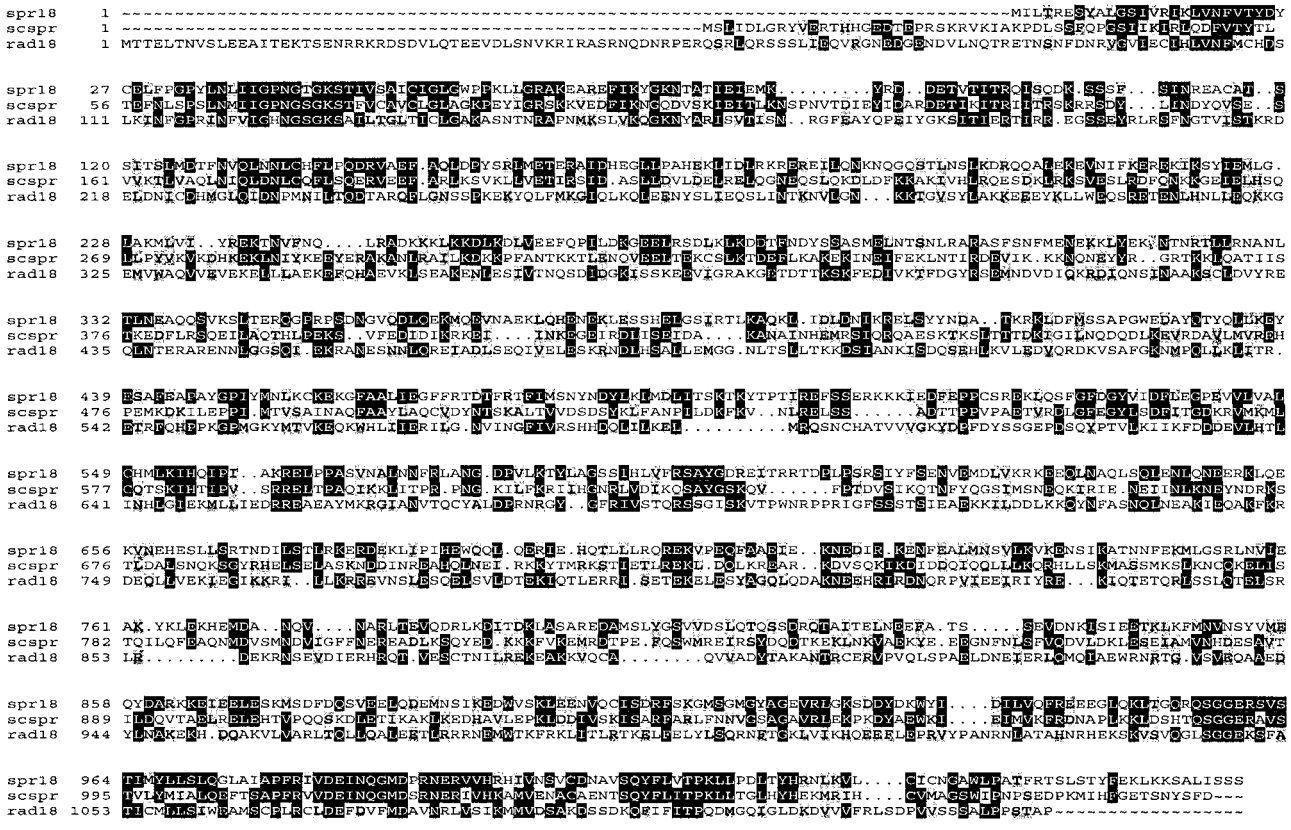

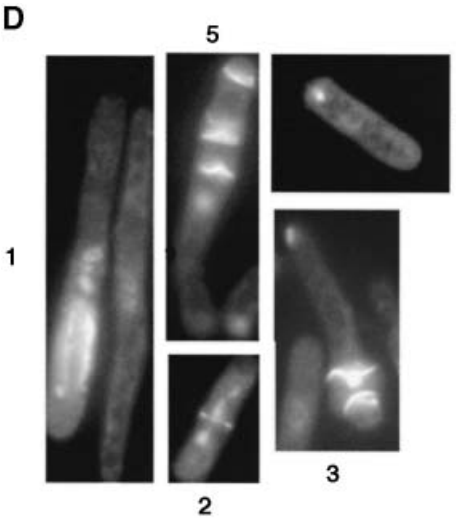
D
1
2
3
4
5

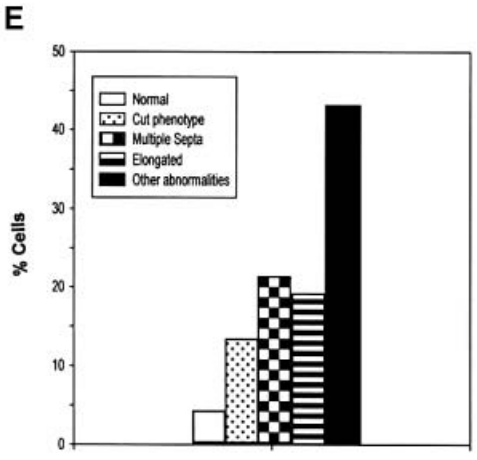
E
% Cells
Normal
Cut phenotype
Multiple Septa
Elongated
Other abnormalities
0
10
20
30
40
50

precipitates were electrophoresed in an SDS–polyacrylamide gel and immunoblotted with the anti-myc antibody. Figure 4C shows that myc-tagged Rad18 co-immunoprecipitated with Spr18 in these experiments in the presence of salt concentrations up to 0.75 M (lanes 1–6). Similar results were obtained when the blots were probed with anti-Spr18 (data not shown). The results were not affected by treatment of the cell extracts with DNase I prior to immunoprecipitation, demonstrating that the interaction was not mediated by binding to DNA. When the immunoprecipitation experiments were carried out with control untagged strain 501, no bands were detected on the immunoblot (Figure 4C, lanes 7 and 8). These results demonstrate that Rad18 and Spr18 do indeed interact, consistent with the idea that the two proteins form a heterodimer in *S.pombe* cells, although we have not formally eliminated the possibility that the interaction might be mediated by another protein. In results to be presented elsewhere, we have shown a similar interaction between the human orthologues of these proteins (E.M.Taylor, J.Moghraby and A.R.Lehmann, unpublished observations).

Spr18 is the p124

The peptide elution fractions from the immuno-affinity column obtained using both the myc-Rad18 and 501 extracts (Figure 3) were analysed by immunoblotting with the anti-Spr antibody. Spr18, like Rad18, was detected in the bound and eluted proteins from the myc-Rad18 extract (Figure 3B, lane 6), but not in the untagged control extracts (lane 8). The band detected using the anti-Spr18 antibody corresponded with that of the p124 protein in the Coomassie-stained gel. These results confirm that p124 is the SMC protein Spr18 and are consistent with the suggestion that Rad18–Spr18 forms a heterodimeric core of a large complex similar to the other SMC complexes, cohesin and condensin. To investigate whether the Rad18–Spr18 complex contains other known DNA damage response genes, we carried out immunoblotting of the proteins eluted from the anti-myc affinity column using a series of antibodies. We were unable to detect the presence of the DNA damage response proteins Rad9, Rad26, Cds1, Rqh1 or Rad21 in the Rad18–Spr18 complex (data not shown).

Spr18 is an essential gene

If Spr18 is the partner protein of Rad18, we anticipated that, like Rad18, it would be an essential gene. We deleted the entire ORF of the *spr18* gene from the genome in a diploid strain by replacing one copy of the gene with the *ura4*$^+$ marker. Following sporulation and plating in the absence of uracil, no haploid colonies were obtained, suggesting that the *spr18* gene was essential for cell proliferation. In order to confirm this, tetrads were dissected from the spores and plated on yeast extract plates. Viability and the Ura4$^+$ phenotype segregated in a 2:0 manner, confirming that s*pr18*, like *rad18* and the *SMC* genes, is essential for cell proliferation. In order to determine the terminal phenotype of the *spr18* deletion strain, the spores were germinated in liquid medium with selection for Ura4$^+$, and cell number and morphology were determined. Germinating spores underwent one or two divisions and ceased growth with a variety of abnormal morphologies. Several examples are shown in Figure 4D. Many cells were elongated, in some cases excessively so (Figure 4D, examples 1 and 5), often with several septa (examples 3 and 5), and the nuclear material was barely detectable, either being present in a single nucleus (example 4) or spread amorphously through part of the cell (example 1). A proportion of cells (10–15%) showed a cut phenotype (Figure 4D, example 2). The distribution of these different phenotypes is shown in Figure 4E. The similarity of the terminal phenotype of the s*pr18* deletion mutant, *rad18* deletion (Lehmann *et al*., 1995) and wild-type cells overexpressing dominant-negative mutants of *rad18* (see below), provides further evidence that Rad18 and Spr18 perform similar functions in the cell.

Mutagenesis of rad18 defines important structural domains

The characteristic SMC structure of Rad18, with globular head and tail regions and two coiled-coil domains separated by a hinge, is depicted schematically in Figure 5A. To gain insight into the roles of the different domains, we have used site-directed mutagenesis to introduce a series of mutations into *rad18* cDNA. The cDNA was cloned under the control of the attenuated thiamine-repressible *nmt1* promoter in the vectors pRep41MH N (Leu$^+$) or pRep42MH N (Ura$^+$) (Maundrell, 1993; Craven *et al*., 1998), so that the Rad18 protein was N-terminally myc-tagged. The effects of the mutations were examined in different ways, as follows: (i) the ability of the mutant plasmids to rescue the lethal effect of a *rad18* deletion was examined by transformation into the *rad18::ura4*$^+$/*rad18*$^+$ diploid strain; (ii) the mutated plasmids were overexpressed in wild-type cells to look for dominant-negative effects of the mutant gene on cell growth and viability, as well as on sensitivity to UV- and γ-irradiation; and (iii) the mutated genes were introduced into *rad18-X* cells and their impact on the sensitivity of the mutant to ionizing and UV-irradiation was examined following their transient overexpression.

The mutations and their effects are summarized in Figure 5 and Table I. Several of the mutant constructs had a dominant-negative effect on cell viability (Figure 5A). The proportion of the population that lost viability depended on the mutation, but the phenotype of the dying cells was quite similar in all cases, and resembled the terminal phenotype of deletion mutants of *rad18* (Lehmann *et al*., 1995) or *spr18* (see above). For simplicity

Fig. 4. Spr18, the SMC partner protein of Rad18. (**A**) Phylogenetic tree of all the SMC family members in *S.cerevisiae* and *S.pombe*. (**B**) Sequence alignments of Rad18 with Spr18 and its *S.cerevisiae* orthologue (designated scspr). Identical amino acids are highlighted in black, and conserved residues are in grey. (**C**) Extracts of myc-Rad18 cells were immunoprecipitated with either anti-myc or anti-Spr18 antibody in the presence of the salt concentrations indicated. The immunoprecipitates were immunoblotted and probed with anti-myc antibody. The right hand lanes (7 and 8) show results with untagged strain 501. (**D**) Terminal phenotypes of the *spr18* deletion mutant. Diploid *spr18*$^+$/*spr18::ura4*$^+$cells were sporulated and grown in the absence of uracil for 36 h. Cells were fixed and stained with DAPI and calcofluor. (**E**) Frequency of different phenotypes after 24 h growth.

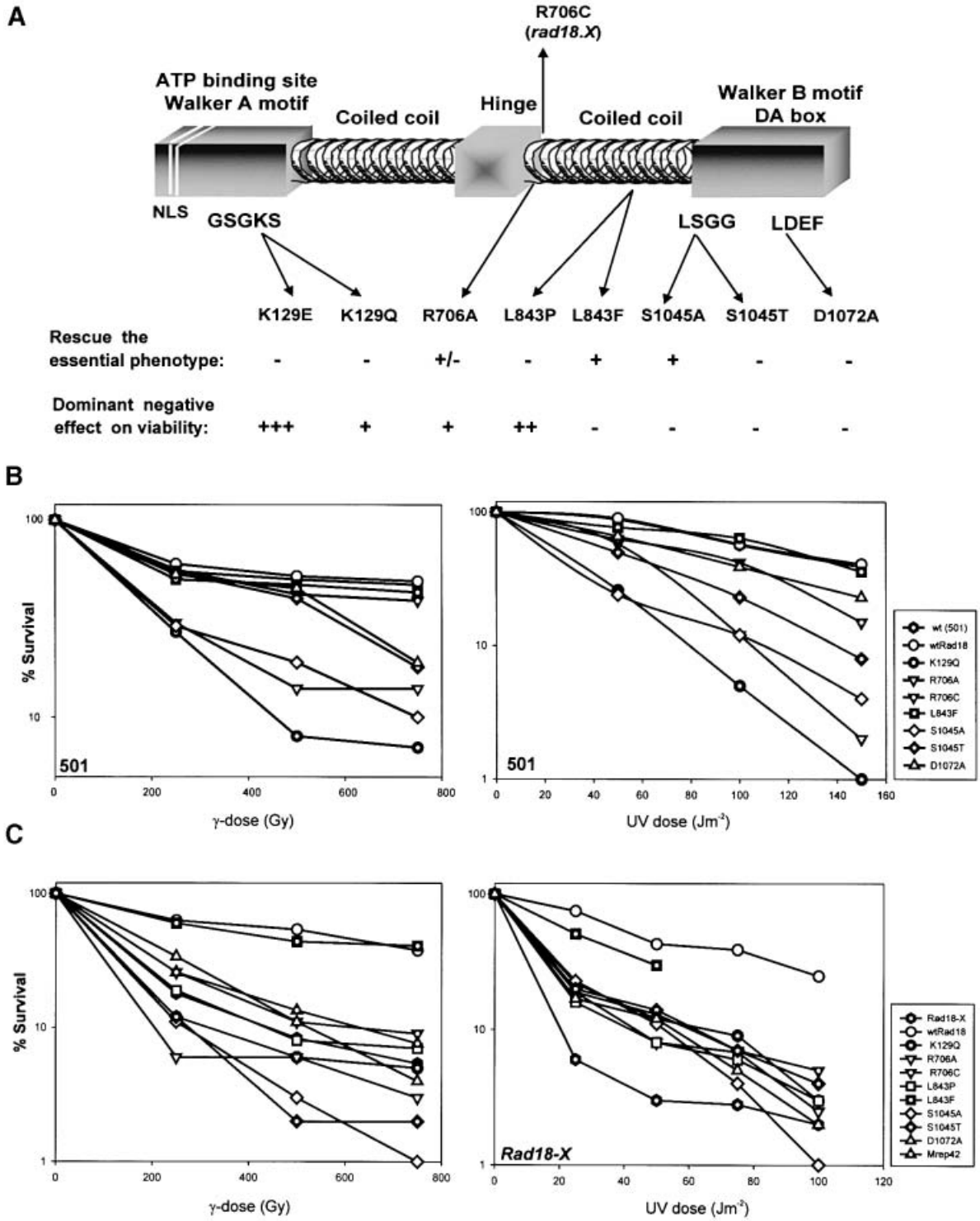

Fig. 5. Effects of site-directed mutations in Rad18. (**A**) Schematic of Rad18 protein with positions of the mutations, their ability to rescue the lethal phenotype of the *rad18* deletion mutant and the effect of their overexpression on the viability of the wild-type strain (+++, all cells dead; ++, most cells dead but a few retain viability; +, 30–40% cells retain viability). (B and C) Survivals after γ- or UV-irradiation of wild-type (**B**) or *rad18-X* cells (**C**) overexpressing the different mutant plasmids. Experiments were carried out three times, typical results are shown (Mrep42, empty pREP42 MH vector).

we will refer to this as the Rad18 phenotype, although there is no intended implication that this phenotype is unique to *rad18* mutants. This phenotype consisted of cells with a variety of abnormal morphologies in which nuclear segregation was clearly aberrant. Many of them were small, a few septated without prior mitosis, resulting in very long cells either without a nucleus or with only one nucleus often with multiple septa. Examples are shown in Figure 6A (compare with overexpressed wild-type *rad18* in Figure 6B).

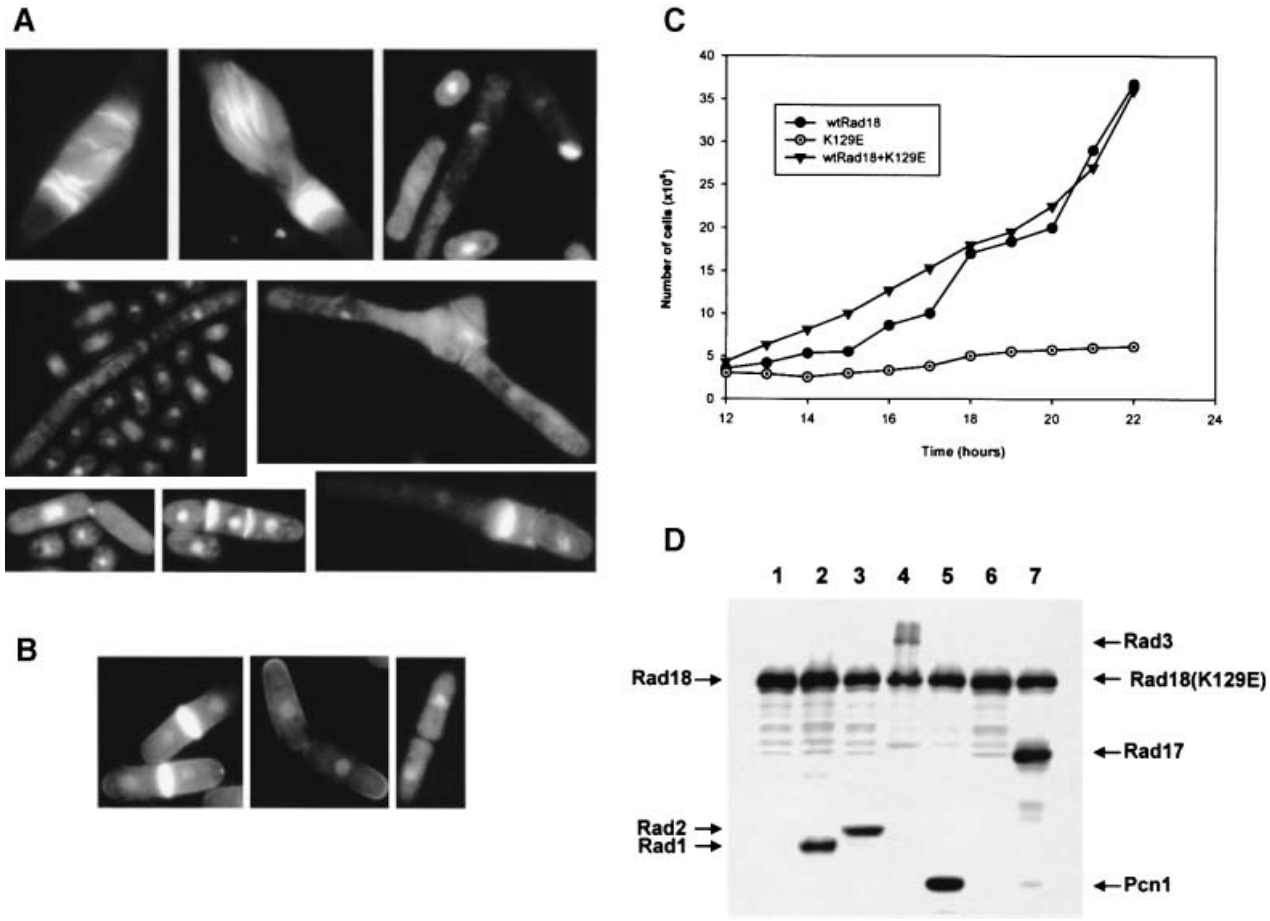

Fig. 6. Dominant-negative effects of mutations in the *rad18* gene. (A and B) Effects of overexpressing (**A**) *rad18K129Q*, *rad18L843P* or *rad18R706A* and (**B**) wild-type *rad18* on cell growth and morphology. (**C**) Wild-type cells overexpressing either wild-type *rad18*, the *rad18K129E* mutant plasmid, or both, were incubated in the absence of thiamine and cell numbers counted over a 24 h time period. (**D**) Western blots from cells overexpressing myc-tagged *rad18K129E* alone (lane 1) or with *myc*-tagged *rad1* (lane 2), *rad2* (lane 3), *rad3* (lane 4), *pcn1* (lane 5), *rad17* (lane 7) and HA-tagged *cdc6* (lane 6).

Table I. Summary of effects of overexpressing mutant constructs

	K129E	K129Q	R706C	R706A	L843P	L843F	S1045A	S1045T	D1072A
WT viability[a]	0	35	+	42	20	+	+	+	+
WT UV[b]	dead	S	N	S	dead	N	S	S	N
WT γ[b]	dead	S	N	S	dead	N	S	N	N
Rad18-X UV[c]	dead	SS	SS	SS	SS	R	SS	SS	SS
Rad18-X γ[c]	dead	SSS	SS	SSS	SS	R	SSS	SSS	SS
Rad18Δ[d]	no	no	yes	partial	no	yes	yes	no	no

[a]Numbers denote percentage of viable cells. +, >70% viability.
[b]N, normal; S, more sensitive than normal.
[c]R, restores wild-type resistance; SS, sensitivity comparable to *rad18-X*; SSS, sensitivity greater than *rad18-X*.
[d]Yes, does; no, does not rescue lethality of deletion strain.

The N-terminal domain of Rad18 contains the highly conserved Walker Type A box found in many ATPases. We mutated the conserved Lys129 residue in the GXGKS motif to glutamic acid (*rad18K129E*). When *rad18K129E* was overexpressed in wild-type cells, it had a dramatic dominant-negative effect on viability, completely abolishing the colony-forming ability of the cells. A similar result has recently been obtained for a different mutation in the ATP-binding site by Verkade *et al*. (1999). When the *rad18K129E* was overexpressed in cells growing in liquid culture, cell growth was prevented (Figure 6C) and the cells died with the Rad18 phenotype.

We also generated a milder mutation of Lys129 to glutamine (K129Q). When plasmids containing this construct were overexpressed in wild-type cells, the resulting colonies were very small, and in liquid culture, a significant proportion of the cells (65%) showed the Rad18 phenotype and had reduced viability (Figure 6A). The viable cells were sensitized to both UV- and ionizing radiation (Figure 5B). The mutant plasmid failed to rescue the

viability of the deletion mutant and slightly increased the sensitivity of the *rad18-X* cells to γ-irradiation (Figure 5A and C).

The C-terminal globular region contains motifs LSGG and DE, conserved in all SMC proteins, the latter probably representing part of the Walker Type B motif involved in ATP–Mg^{2+} binding. We mutated Ser1045 from the LSGG sequence to either alanine or threonine (*rad18S1045A* or *rad18S1045T*), and Asp1072 to alanine (*rad18D1072A*). Overexpression of these mutated genes had no significant effect on the viability of wild-type cells. However, the *rad18S1045A* mutant plasmid sensitized the cells to both γ- and UV-irradiation damage, whereas *rad18S1045T* had less effect and *rad18D1072A* had minimal effect (Figure 5B). The S1045A and S1045T plasmids slightly increased the γ-irradiation sensitivity of the *rad18-X* mutant (Figure 5C). Importantly, however, the *rad18S1045A* mutant plasmid, but neither of the others, was able to rescue the lethality of the *rad18* deletion strain (Figure 5A). This significant result shows that the S1045A mutation is able to separate the repair from the essential phenotype of the cells. It is possible that the *rad18* mutant plasmid rescued the *rad18* deletion because the mutant gene was overexpressed. However, in results to be presented in detail elsewhere, we have eliminated this possibility. We have integrated the S1045A mutation into the genomic *rad18* gene, in which it is expressed at normal levels. This strain is viable and sensitive to radiation.

Coiled-coil motifs are amphipathic α-helices characterized by heptad repeats with hydrophobic amino acids at the first and fourth residues of each heptad (Lupas *et al*., 1991). We mutated Leu843, in the middle of a long heptad repeat, either to proline (L843P), which would be expected to destroy the coiled-coil structure, or to phenylalanine (L843F), which is hydrophobic like leucine, but has a completely different structure. The latter mutation behaved like wild type in all respects (Figure 5B): it restored viability to the *rad18* deletion strain and rescued the sensitivity to DNA damage of the *rad18-X* cells (Figure 5C). In contrast, L843P had a dramatic effect. Only a few wild-type cells overexpressing the plasmid were able to form colonies, which were very small, and in liquid culture, most of the cells (80%) had the Rad18 phenotype. Viability of the deletion strain was not restored with this mutant plasmid.

The mutation in *rad18-X*, which is sensitive to UV- and γ-irradiation and elevated temperatures, results in the change R706C. We considered the possibility that this change might exert its effects because the mutant protein contains a cysteine residue, which might form aberrant disulfide bridges. We therefore mutated Arg706 to alanine (R706A) and compared its effects with those of R706C. Overexpression of R706C had no effect on either wild-type or *rad18-X* cells and restored the viability of the deletion strain. The effects of R706A were, however, more severe, the phenotype being quite similar to that of *rad18K129Q* (see Figure 5B and C and Table I). These findings ruled out the possibility that the phenotype of *rad18-X* resulted from aberrant disulfide bridges, and rather implicated R706 as an important residue for Rad18 function.

In summary, we have found a gradation in severity of mutations in *rad18*. Mutations in the ATP-binding site in the N-terminus and disruption of the coiled-coil domain had the most dramatic effects, suggesting that the ATP-binding site and coiled-coil structures are essential for all functions. Effects of mutations in the conserved C-terminal domain were less severe. The S1045A mutation in the conserved LSGG motif enabled us to separate repair from essential functions of the protein, since it only affected the former.

Overexpression of damage response genes rescues the dominant-negative phenotype

We have looked for genetic interactions between *rad18* and other genes by examining their ability to suppress the dominant-negative effects of the K129E mutation in the ATP-binding site. If the normal and mutant cDNAs were co-overexpressed from separate plasmids with the same *nmt1* promoter (in pRep41 and 42), the normal plasmid was able to rescue the growth-inhibitory effects of the mutant plasmid (Figure 6C). We used this co-expression system to investigate whether several other genes (*rad1*, *rad2*, *rad3*, *rad17*, *pcn1* and *cdc6*) could also rescue the adverse effects of the mutant plasmid. We found that when either the cell cycle checkpoint genes *rad1* or *rad3*, the *rad2* gene encoding a structure-specific nuclease or the *cdc6* gene encoding DNA polymerase δ was overexpressed together with *rad18K129E*, the growth inhibition was overcome, whereas *pcn1* encoding PCNA and the checkpoint gene *rad17* had no effect. In order to ensure that this was not merely the result of the second plasmid reducing the expression of the mutant gene, we used Western blotting to determine the levels of expression after 14 h in the absence of thiamine. Since the genes were also myc-tagged (in most cases), we were able to detect both Rad18 and the co-expressing proteins using an antibody directed against the myc epitope tag. The expression of the mutant *rad18K129E* was not affected by co-expression from the second plasmid (Figure 6D). Our data therefore provide evidence for a genetic interaction between *rad18* and *rad1*, *rad2*, *rad3* and *cdc6*. These interactions will be studied in detail in future work.

Discussion

Rad18–Spr18 and other SMC protein complexes

Although our understanding of many DNA repair processes has increased dramatically over the last few years, the functions of many DNA repair proteins are still poorly understood. As shown by the scheme in Figure 1, Rad18 plays an important role in several repair processes, but its exact function is unknown. The other SMC protein family members are essential for chromosome condensation (SMC2 and 4) and cohesion (SMC1 and 3) (see Hirano, 1998; Jessberger *et al*., 1998), although the role that these proteins play at the molecular level is poorly understood. We have shown in this paper that Rad18 resembles other SMC proteins in that it forms a heterodimeric complex with a closely related partner protein, Spr18, and Rad18–Spr18 is part of a higher molecular weight complex. This complex has a molecular weight >1 MDa, is stable in high salt, contains at least five other proteins and has DNA-stimulated ATPase activity. Similarly, the condensins from *Xenopus* and *S.pombe* contain multiple subunits

including, in *Xenopus*, XCAP-C and XCAP-E (Hirano *et al*., 1997) and in *S.pombe*, Cut3 and Cut14 (Tanaka *et al*., 1999), the orthologues of SMC2 and SMC4. Likewise the cohesins, which include SMC1 and SMC3 (Losada *et al*., 1998), and the dosage compensation complex from *Caenorhabditis elegans*, which contains the SMC protein DPY27 (Chuang *et al*., 1996), also contain multiple subunits. A complex designated RC-1, which was able to carry out strand exchange reactions, is composed of bovine SMC1 and SMC3 together with DNA polymerase ε and DNA ligase III (Jessberger *et al*., 1996). Both Rad18 and Spr18 have orthologues in the *S.cerevisiae* and *C.elegans* databases and we have isolated human orthologues of both (E.M.Taylor, J.Moghraby and A.R.Lehmann, unpublished results). In view of the similarity in structural composition between the Rad18–Spr18 complex, condensin and cohesin, we consider Rad18–Spr18 to be the third conserved SMC complex in eukaryotes.

Structure–function relationships in Rad18

Structural studies on bacterial SMC-like proteins have been carried out recently by Melby and coworkers (Melby *et al*., 1998). MukB is the only SMC-like protein in *Escherichia coli* and has an antiparallel homodimeric structure, with the globular domains attached by rigid coiled-coil domains to the hinge. The coiled-coil regions form the basis for the dimerization. The hinge appeared quite flexible, permitting a scissoring movement. It is probable that in the Rad18 complex, Rad18 and Spr18 form antiparallel heterodimers.

Site-directed mutagenesis studies (Figures 5 and 6) have shown that the globular N-terminal domain and the coiled-coil regions are required for both repair and essential functions of Rad18. This is consistent with the structure suggested above. If we assume that Rad18 forms a similar structure but as a heterodimer with Spr18, we can provide a ready explanation for the dominant-negative effects of overexpressed mutant Rad18 (Figure 6 and Verkade *et al*., 1999). In the majority of the mutants in which the coiled-coil domains remain intact, the overexpressed mutant Rad18 protein will dimerize and thereby sequester the cellular Spr18, preventing it from dimerizing with the endogenous protein. The L843P mutant probably causes local disruption of the α-helical structure of the more C-terminal coiled coil, but the more N-terminal coiled-coil domain is likely to be unaffected and still capable of interacting with Spr18.

Interestingly, mutations in the conserved C-terminal globular domain had relatively mild effects. Particularly interesting is the S1045A mutation (Figure 5), which destroyed the repair function of the protein, whilst retaining its essential function. This was quite surprising in view of the fact that the motif LSGG, encompassing Ser1045, is conserved in all SMC proteins (with the exception of Spr18, which contains the sequence QSGG). It is also found in a large family of ATP transporter proteins (Ames *et al*., 1992), in which it has been proposed that the LSGG motif forms an important linker region between different domains. In the latter protein family the serine residue is essential for the transporter function of the *S.cerevisiae* Ste6p protein involved in transport of the a-factor pheromone (Browne *et al*., 1996), and it is mutated in the CFTR protein in several cystic fibrosis patients (Kerem *et al*., 1990; Gregory *et al*., 1991). This mutation provides an opportunity for further investigation of the repair functions of Rad18 and its homologues.

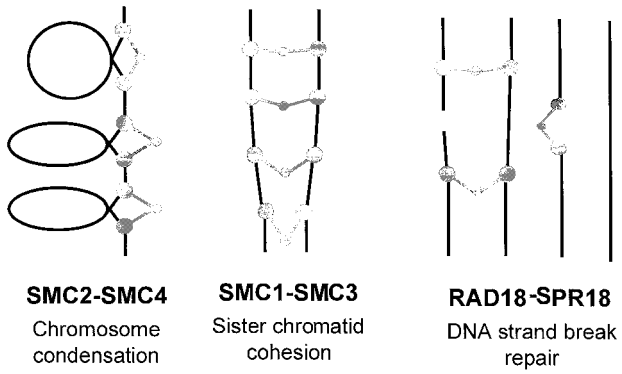

Fig. 7. Models for involvement of the Rad18–Spr18 complex in DNA repair. The diagram shows the roles of SMC proteins in chromosome condensation and cohesion as proposed by Hirano (1999), and two possible roles for Rad18–Spr18 in repair of double-strand breaks. Black lines represent double-stranded DNA, and the grey symbols represent SMC proteins with globular N- and C-termini and hinge regions, with extended coiled coils in between.

Function of the Rad18–Spr18 complex

The SMC protein complexes function in chromosome-associated processes, such as condensation, cohesion and dosage compensation. It is thought that the putative scissoring action, which is possible because of the flexibility of the SMC dimer (Melby *et al*., 1998), enables the complexes to move DNA molecules relative to each other or to other cellular structures. The condensin complex from *Xenopus* is able to supercoil DNA in the presence of topoisomerase I (Kimura and Hirano, 1997) and to effect topological reconfigurations of DNA molecules (Kimura *et al*., 1999). The *S.cerevisiae* SMC1p and SMC2p proteins are able to bind to DNA, and this DNA-binding activity resides in the C-terminus of the molecule (Akhmedov *et al*., 1998). We find that Rad18 binds tightly to DNA-cellulose columns (our unpublished data), suggesting that Rad18 is likely to be a DNA-binding protein, which would be consistent with the DNA-stimulated ATPase activity that we have found associated with the Rad18–Spr18 complex. We previously suggested that Rad18 was involved in recombinational repair processes (Lehmann *et al*., 1995). Our current work together with published data on the functions of SMC proteins lead us to speculate that the function of the Rad18–Spr18 complex is to bring together and/or hold broken DNA molecules together in the vicinity of double-strand damage to allow repair by recombination to take place (see Figure 7). Such damage could be either a double-strand break produced directly by ionizing radiation, or a UV photoproduct opposite a gap or stalled replication fork generated during replication of UV damage. We envisage that the Rad18–Spr18 complex either holds the ends of the break together or alternatively holds the broken chromosome in register with its sister or homologue to allow the Rhp51 RecA homologue to initiate strand exchange. In this context the Rad18–Spr18 complex presumably plays a complementary role to the cohesins, which are known to hold sister chromatids together, and are also required for a normal response to radiation, since mutants in *S.pombe rad21*, a

non-SMC component of cohesin, are sensitive to radiation. Recent data suggest that the cohesin complex is present at specific sites along the chromosome arms rather than coating the lengths of the chromosomes (Blat and Kleckner, 1999; Tanaka *et al*., 1999). In the context of recombinational repair of double-strand DNA damage, it may be that cohesins are necessary to maintain the overall cohesion of the sister chromatids, whereas the Rad18–Spr18 complex has a more specific role at sites of damage. The suggestion of a role for Rad18 in recombination is supported by the 4-fold reduction in intrachromosomal recombination recently reported in a *Rad18* mutant of *Arabidopsis thaliana* (Mengiste *et al*., 1999). A more complex role for Rad18 in response to DNA damage has been suggested by the work of Verkade *et al*. (1999), who provided evidence to suggest that under some circumstances Rad18 was required to maintain a checkpoint following DNA damage, although establishment of the checkpoint was clearly normal. Our finding of a genetic interaction between some of the checkpoint genes and *rad18* is consistent with these observations. We obtained no evidence, however, for physical association in the Rad18–Spr18 complex of several checkpoint proteins tested. The relationship of Rad18 to the checkpoint machinery is likely, therefore, to be complex and indirect.

Both Rad18 and Spr18 are essential for cell proliferation. Our results in Figure 4D and Figure 6 show that in the absence of functional Spr18, or when dominant-negative mutant *rad18* constructs are overexpressed, cells appear to be unable to replicate their DNA, but nevertheless they continue to grow, lay down septa and develop grossly abnormal morphologies. This is indicative of a role both in DNA replication and in mitotic control. Occasional double-strand breaks occur during DNA replication and these are thought to be repaired by recombination. Cells deficient in the recombination-repair genes *rhp51* or *rhp54* grow poorly (Muris *et al*., 1993, 1996), presumably because they have difficulty in dealing with damage arising during replication. Double mutants of *rhp51* or *rhp54* with the DNA damage checkpoint genes are inviable (Muris *et al*., 1996), showing that checkpoint-mediated mitotic delay is necessary for the cell to deal with this kind of replicative stress. We propose that the inviability of *rad18* and *spr18* mutants arises from their involvement in linking replication, repair and mitotic control. Further work will be necessary to unravel the origin of these complex phenotypes.

Materials and methods

Antibodies

The 9E10 anti-myc monoclonal antibody used for immunoblotting was obtained from Santa Cruz. For immuno-affinity chromatography we used supernatants from CRL-1729 hybridoma cells obtained from the American Type Culture Collection, and cultured in RPMI with 10% fetal calf serum. The supernatant was bound to protein G–agarose, extensively washed and covalently crosslinked using dimethylpimelimidate (Harlow and Lane, 1988). Polyclonal antibodies to Rad18 and Spr18 protein were raised in sheep against the peptides VYSLAKKEEEYKLLWEQSRE and RKRERELQNKNQGQSTLNSLKDR, respectively. These antibodies identified the corresponding *in vitro* translated proteins. They also detected proteins of the appropriate size in cell extracts, which were not detected by the corresponding pre-immune sera. Antibodies against other damage response proteins were generously supplied by Drs T.Caspari, J.Murray and A.M.Carr.

Immunoprecipitation

For these experiments we constructed an *S.pombe* strain *myc*-tagged in the genome (myc-Rad18). A fragment of DNA containing 950 bp of *rad18* upstream sequence and the coding sequence up to the *Nco*I site at nt 1760 was cloned into the integrating vector pSta18 (Carr *et al*., 1989), which contains the *sup3.5* $tRNA^{Ser}_{UGA}$ insert (Hottinger, 1982). The His_6-myc_2 coding sequence was inserted as an *Nde*I fragment from pGEMMH (Craven *et al*., 1998) into an *Nde*I site engineered at the start of the *rad18* ORF. This plasmid was transformed into *S.pombe* strain 501 (*leu1.32 ura4.D18 ade6.704*) and selection was applied for growth in the absence of adenine. (The *ade6.704* mutation in the 501 strain is suppressed by *sup3.5*.) Ade^+ colonies were grown and analysed for the integration of the tagged sequence by Southern blotting and immunoblotting. A similar procedure was followed for the *S.pombe rad18-X myc*-tagged strain (myc-Rad18-X).

For immunoprecipitations, crude extract containing 2 mg of total protein was incubated overnight with either the anti-Spr18 antibody or the 9E10 anti-myc antibody in ab binding buffer [40 mM HEPES pH 7.8, 2 mM EDTA, 2 mM EGTA, 60 mM β-glycerophosphate, 1 mM NaF, 0.5 mM phenylmethylsulfonyl fluoride (PMSF), 0.2 mM dithiothreitol (DTT), 0.1 mM orthovanadate, 10% glycerol and protease inhibitor cocktail, as described below] in the presence of different concentrations of NaCl. The immune complexes were captured on protein G–agarose beads, washed several times, boiled with gel loading buffer and electrophoresed in 10% SDS–PAGE gels. They were blotted onto PVDF membrane filters and probed with the anti-myc antibody.

Purification of the Rad18 complex

For purification, 30 l of exponentially growing myc-Rad18 cells were harvested, washed and the cell pellet resuspended in an equal volume of lysis buffer A (40 mM HEPES pH 7.8, 0.4 M KCl, 80 mM β-glycerophosphate, 12 mM NaF, 5 mM EGTA, 5 mM EDTA, 1 mM DTT, 1 mM PMSF, 0.1 mM orthovanadate, 10% glycerol, and a protease inhibitor cocktail consisting of 5 μg/ml each of trypsin inhibitor, pepstatin, leupeptin, aprotinin, 10 μg/ml bestatin and E-64, and 50 μg/ml chymotrypsin inhibitor). The cells were snap-frozen in liquid nitrogen and lysed using a blender, following addition of copious quantities of dry ice. The lysate was clarified by centrifugation and subjected to ammonium sulfate precipitation. The 15–45% cut containing the Rad18 protein was dissolved in lysis buffer and dialysed overnight against the same buffer. The extract containing ~300 mg of protein was applied in multiple injections to a Superdex 200, 10/30 FPLC column (Pharmacia Biotech). Fractions of 0.25 ml were collected and analysed by Western blotting using the anti-myc monoclonal antibody. The high-molecular-weight fractions containing the Rad18 protein were pooled and fractionated on heparin–Sepharose Cl-6B (Pharmacia Biotech) equilibrated in buffer B/0.1 M KCl (25 mM HEPES pH 7.8, 2 mM EGTA, 3 mM $MgCl_2$, 0.1 mM DTT, 0.5 mM PMSF, 12% glycerol). After extensive washing, proteins were eluted with buffer B/0.2, 0.4, 0.6 and 1 M KCl. The 0.6 M KCl eluate that contained the Rad18 protein was incubated overnight at 4°C with protein G–agarose beads (Pharmacia Biotech) crosslinked with anti-myc antibody in buffer B/0.3 M KCl, containing 0.4 mM EDTA and protease inhibitor cocktail. The beads were washed once with the same buffer, four times in 10 vol. of buffer B/0.5 M KCl, 0.1% NP-40, and twice in buffer B/0.1 M KCl, 0.01% NP-40. Bound proteins were eluted twice at 30°C for 1 h each with peptide corresponding to the myc epitope (AEEQKLISEEDL) at 3 mg/ml in buffer B/0.1 M KCl, 0.2 mg/ml insulin and 1 μg/ml aprotinin and E64. The eluted fractions were dialysed twice in buffer B containing 0.1 M KCl and 15% glycerol to eliminate the peptide. The proteins were separated on 10% SDS–PAGE and stained with colloidal Coomassie Brilliant Blue (Brilliant Blue G, colloidal concentrate; Sigma). Alternatively they were analysed by immunoblotting with antibodies specific for different DNA damage response proteins.

In experiments to estimate the size of the complex, pooled Superdex 200 fractions that contained the high-molecular-weight peak, derived as above, were further subjected to gel filtration on a Superose 6 FPLC column (Pharmacia Biotech). In this case 0.5 ml fractions were collected and analysed by Western blotting. The column was calibrated with HMW Gel Filtration Calibration Markers (Pharmacia Biotech).

ATPase assay

For assaying ATPase activity, elution from the affinity column with the myc peptide was carried out at 30°C for 20 min only, and the eluate was dialysed against buffer B containing 0.05 M KCl. Protein eluates were then incubated for 2 h at 30°C in the presence of 0.1 μCi [γ-^{32}P]ATP (7000 Ci/mmol; ICN) in a 10 μl reaction volume containing 25 mM

Tris–HCl pH 7.5, 4 mM $MgCl_2$, 20 µM ATP, 1 mM DTT and 50 µg/ml BSA. The reaction was stopped by adding 5 µl of 0.5 M EDTA pH 8.0. One microlitre of each reaction mixture was then spotted on a PEI-cellulose thin layer chromatography (TLC) plate (Sigma) and developed in 0.75 M KH_2PO_4. Radiolabelled ATP and inorganic phosphate were quantitated on a Storm 840 PhosphorImager (Molecular Dynamics). DNA-dependent ATPase activity was assayed in the presence or absence of double- or single-stranded DNA at a final concentration of 15 ng/µl.

Site-directed mutagenesis

A *rad18* cDNA clone was constructed by PCR and subcloning from total *S.pombe* cDNA. The internal *Nde*I site was destroyed by site-directed mutagenesis, and after removing PCR errors by further mutagenesis, the cDNA was cloned as an *Nde*I–*Sal*I fragment into the pRep41 MH, and pRep42 MH epitope-tagging expression vectors (Craven *et al*., 1998). Mutations in the cDNA were introduced at specific sites using the procedure of Kunkel *et al*. (1987), and all the mutant clones were sequenced completely to ensure that only the desired mutations had been introduced. We regularly found that subcloning of *rad18* constructs was unsuccessful when the ligated DNA was transformed into a variety of commonly used *E.coli* strains. We therefore transformed the ligation mixes directly into *S.pombe* and successfully obtained the desired products.

Cell survival and complementation of the essential phenotype

Mutant constructs were introduced either into wild-type or *rad18-X* cells in the presence of thiamine to maintain the *nmt1* promoter on the plasmid in the repressed state. For survival experiments, cells were grown in the absence of thiamine for 16 h to induce steady levels of expression from the *nmt1* promoter. They were then exposed to UV- or γ-irradiation and 1000 cells were plated out as described previously (Lehmann *et al*., 1995). Wild-type cells were plated on minimal medium, and *rad18-X* on YEP. For effects on cell viability, wild-type cells were grown for 12 h in the absence of thiamine. Samples were then plated both in the presence and absence of thiamine. Other samples were taken every hour for the next 14 h and the cells were counted, fixed in methanol and stained with DAPI and calcofluor.

To investigate the ability of the mutant constructs to rescue the inviability of a *rad18* deletion, *rad18* mutants in pRep41MH (Leu^+) (Craven *et al*., 1998) were transformed into the *rad18*$^+$*/rad18::ura4* diploid strain in the presence of thiamine. Colonies were picked and induced to sporulate by growth on low nitrogen plates. The spores were digested with helicase, and plated (without thiamine) in the absence of leucine, or in the absence of both uracil and leucine. Rescue of the deletion strain was indicated by growth in the absence of both uracil and leucine.

Acknowledgements

We are indebted to Antony Carr for continued help, advice and instruction, to Jo Murray for rad18 cDNA plasmids, and to Antony Carr, Penny Jeggo, Elaine Taylor and Patricia Kannouche for comments on the manuscript. This work was supported in part by EC contracts CHX-CT94-0443 and F14P-CT95-0010.

References

Akhmedov,A.T., Frei,C., Tsai-Pflugfelder,M., Kemper,B., Gasser,S.M. and Jessberger,R. (1998) Structural maintenance of chromosomes protein C-terminal domains bind preferentially to DNA with secondary structure. *J. Biol. Chem.*, **273**, 24088–24094.

Ames,G.F.-L., Mimura,C.S., Holbrook,S.R. and Shyamata,V. (1992) Traffic ATPases: a superfamily of transport proteins operating from *Escherichia coli* to humans. *Adv. Enzymol.*, **65**, 1–47.

Avery,A.M., Kaur,B., Taylor,J.S., Mello,J.A., Essigmann,J.M. and Doetsch,P.W. (1999) Substrate specificity of ultraviolet DNA endonuclease (UVDE/Uve1p) from *Schizosaccharomyces pombe*. *Nucleic Acids Res*., **27**, 2256–2264.

Blat,Y. and Kleckner,N. (1999) Cohesins bind to preferential sites along yeast chromosome III, with differential regulation along arms versus the centric region. *Cell*, **98**, 249–259.

Browne,B.L., McClendon,V. and Bedwell,D.M. (1996) Mutations within the first LSGGQ motif of Ste6p cause defects in a-factor transport and mating in *Saccharomyces cerevisiae*. *J. Bacteriol*., **178**, 1712–1719.

Carr,A., MacNeil,S.A., Hayles,J. and Nurse,P. (1989) Molecular cloning and sequence analysis of mutant alleles of the fission yeast cdc2 protein kinase gene: implications for cdc2+ protein structure and function. *Mol. Gen. Genet.*, **218**, 41–49.

Caspari,T. and Carr,A.M. (1999) DNA structure checkpoint pathways in *Schizosaccharomyces pombe*. *Biochimie*, **81**, 173–181.

Chuang,P., Lieb,J.D. and Meyer,B.J. (1996) Sex-specific assembly of a dosage compensation complex on the nematode X chromosome. *Science*, **274**, 1736–1739.

Craven,R.A., Griffiths,D.J.F., Sheldrick,K.S., Randall,R.E., Hagan,I.M. and Carr,A.M. (1998) Vectors for the expression of tagged proteins in *Schizosaccharomyces pombe*. *Gene*, **221**, 59–68.

Gregory,R.J., Rich,D.P., Cheng,S.H., Souza,D.W., Paul,S., Manavalan,P., Anderson,M.P., Welsh,M.J. and Smith,A.E. (1991) Maturation and function of cystic fibrosis transmembrane conductance regulator variants bearing mutations in putative nucleotide-binding domains 1 and 2. *Mol. Cell. Biol.*, **11**, 3886–3893.

Harlow,E. and Lane,D. (1988) *Antibodies*. Cold Spring Harbor Laboratory Press, Cold Spring Harbor, NY.

Hirano,T. (1998) SMC protein complexes and higher-order chromosome dynamics. *Curr. Opin. Cell Biol.*, **10**, 317–322.

Hirano,T. (1999) SMC-mediated chromosome mechanics: a conserved scheme from bacteria to vertebrates? *Genes Dev.*, **13**, 11–19.

Hirano,T., Kobayashi,R. and Hirano,M. (1997) Condensins, chromosome condensation protein complexes containing XCAP-C, XCAP-E and a *Xenopus* homolog of the *Drosophila* barren protein. *Cell*, **89**, 511–521.

Hottinger,H., Pearson,D., Yamao,F., Gamulin,V., Cooley,L., Cooper,T. and Soll,D. (1982) Nonsense suppression in *Schizosaccharomyces pombe*: the *S. pombe Sup3-e* $tRNA^{Ser}_{UGA}$ gene is active in *S. cerevisiae*. *Mol. Gen. Genet*., **188**, 219–224.

Jessberger,R., Riwar,B., Beachtold,H. and Akhmedov,A.T. (1996) SMC proteins constitute two subunits of the mammalian recombination complex RC-1. *EMBO J.*, **15**, 4061–4068.

Jessberger,R., Frei,C. and Gasser,S.M. (1998) Chromosome dynamics: the SMC protein family. *Curr. Opin. Genet. Dev.*, **8**, 254–259.

Kerem,B.S. *et al*. (1990) Identification of mutations in regions corresponding to the two putative nucleotide (ATP)-binding folds of the cystic fibrosis gene. *Proc. Natl Acad. Sci. USA*, **87**, 8447–8451.

Kimura,K. and Hirano,T. (1997) ATP-dependent positive supercoiling of DNA by 13S condensin: a biochemical implication for chromosome condensation. *Cell*, **90**, 625–634.

Kimura,K., Rybenkov,V.V., Crisona,N.J., Hirano,T. and Cozzarelli,N.R. (1999) 13S condensin actively reconfigures DNA by introducing global positive writhe: implications for chromosome condensation. *Cell*, **98**, 239–248.

Kunkel,T.A., Roberts,J.D. and Zakour,R.A. (1987) Rapid and efficient site specific mutagenesis without phenotypic selection. *Methods Enzymol.*, **154**, 367–368.

Lehmann,A.R. (1996) Molecular biology of DNA repair in the fission yeast *Schizosaccharomyces pombe*. *Mutat. Res.*, **363**, 147–161.

Lehmann,A.R., Walicka,M., Griffiths,D.J.F., Murray,J.M., Watts,F.Z., McCready,S. and Carr,A.M. (1995) The *rad18* gene of *Schizosaccharomyces pombe* defines a new subgroup of the SMC superfamily involved in DNA repair. *Mol. Cell. Biol.*, **15**, 7067–7080.

Losada,A., Hirano,M. and Hirano,T. (1998) Identification of *Xenopus* SMC protein complexes required for sister chromatid cohesion. *Genes Dev.*, **12**, 1986–1997.

Lupas,A., Van Dyke,M. and Stock,J. (1991) Predicting coiled coils from protein sequences. *Science*, **252**, 1162–1164.

Maundrell,K. (1993) Thiamine-repressible expression vectors pREP and pRIP for fission yeast. *Gene*, **123**, 127–130.

Melby,T.E., Ciampaglio,C.N., Briscoe,G. and Erickson,H.P. (1998) The symmetrical structure of structural maintenance of chromosomes (SMC) and MukB proteins: long, antiparallel coiled coils, folded at a flexible hinge. *J. Cell Biol.*, **142**, 1595–1604.

Mengiste,T., Revenkova,E., Bechtold,N. and Paszkowski,J. (1999) An SMC-like protein is required for efficient homologous recombination in *Arabidopsis*. *EMBO J.*, **18**, 4505–4512.

Michaelis,C., Ciosk,R. and Nasmyth,K. (1997) Cohesins: chromosomal proteins that prevent premature separation of sister chromatids. *Cell*, **91**, 35–45.

Muris,D.F.R., Vreeden,K., Carr,A.M., Broughton,B.C., Lehmann,A.R., Lohman,P.H.M. and Pastink,A. (1993) Cloning the *RAD51* homologue of *Schizosaccharomyces pombe*. *Nucleic Acids Res.*, **21**, 4586–4591.

Muris,D.F.R., Vreeken,K., Carr,A.M., Smidt,C., Lohman,P.H.M. and Pastink,A. (1996) Isolation of the *Schizosaccharomyces pombe RAD54* homolog, *rhp54*$^{+}$, a gene involved in the repair of radiation damage and replication fidelity. *J. Cell Sci.*, **109**, 73–81.

Murray,J.M., Lindsay,H.D., Munday,C.A. and Carr,A.M. (1997) Role of *Schizosaccharomyces pombe* RecQ homolog, recombination and checkpoint genes in UV damage tolerance. *Mol. Cell. Biol.*, **17**, 6868–6875.

Sutani,T., Yuasa,T., Tomonaga,T., Dohmae,N., Takio,K. and Yanagida,M. (1999) Fission yeast condensin complex: essential roles of non-SMC subunits for condensation and Cdc2 phosphorylation of Cut3/SMC4. *Genes Dev.*, **13**, 2271–2283.

Tanaka,T., Cosma,M.P., Wirth,K. and Nasmyth,K. (1999) Identification of cohesin association sites at centromeres and along chromosome arms. *Cell*, **98**, 847–858.

Verkade,H.M., Bugg,S.J., Lindsay,H.D., Carr,A.M. and O'Connell,M.J. (1999) Rad18 is required for DNA repair and checkpoint responses in fission yeast. *Mol. Biol. Cell*, **10**, 2905–2918.

Yasui,A. and McCready,S.J. (1998) Alternative repair pathways for UV-induced DNA damage. *BioEssays*, **20**, 291–297.

Yonemasu,R., McCready,S., Murray,J.M., Osman,F., Takao,M., Yamamoto,K., Lehmann,A.R. and Yasui,A. (1997) Characterization of the alternative excision repair pathway of UV-damaged DNA in *Schizosaccharomyces pombe. Nucleic Acids Res.*, **25**, 1553–1558.

Yoon,J.H., Swiderski,P.M., Kaplan,B.E., Takao,M., Yasui,A., Shen,B. and Pfeifer,G.P. (1999) Processing of UV damage *in vitro* by FEN-1 proteins as part of an alternative DNA excision repair pathway. *Biochemistry*, **38**, 4809–4817.

Received January 19, 2000; revised and accepted February 16, 2000